Supporting Information

Tailoring electrolyte activity for highly stable LiOH redox process in lithium-oxygen batteries

Jiacheng Yang, Jiasen Guo, Zihong Wang, Bing-Qing Xiong, Jun Ma, Dazhuang Wang, Xiaodi Ren*

Hefei National Research Center for Physical Sciences at the Microscale, CAS Key Laboratory of Materials for Energy Conversion, Department of Materials Science and Engineering, University of Science and Technology of China

Hefei, 230026, China

*E-mail: xdren@ustc.edu.cn

Experimental Sections

Materials

Tetramethylene glycol dimethyl ether (TEGDME, 99%, Aldrich) and dimethyl sulfoxide (DMSO, ≥99.9%, Sigma-Aldrich) were dried by 4 Å molecular sieves. The water contents of the electrolyte solutions were found to be below 20 ppm by Karl Fischer titration (Metrohm 917 titrator). 1-Methyl-3-propylimidazolium Bis(trifluoromethanesulfonyl)imide (C_3C_1im TFSI), and Lithium bis(trifluoromethanesulfonyl)imide (LiTFSI, 99.9%, bidepharm) were dried at 110 °C under vacuum for 24 h before use. Other cell components, such as the glass fiber separator (Whatman, GF/D), carbon paper (H23 CP, Freudenberg), and stainless-steel mesh (SS mesh, 200 mesh), were also dried at 110 °C under vacuum for 12 h before use. The electrolyte solutions were prepared in an Argon-filled glovebox (<0.1 ppm of O_2 and 0.1 ppm of H_2O). Acrylamide (AM, 99%, Aldrich), hexafluorobutyl acrylate (HFBA, 96%, Aldrich) and azobisisobutyronitrile (AIBN, 99%, Aldrich) were used as received without further purification.

Preparation of PAM-b-PHFBA coated Li

AM and HFBA were mixed in the molar ratio of AM:HFBA = 75%. In a weight ratio of 2:1, the HFBA and N-methylpyrrolidone (NMP) were added to the mixture, followed by AIBN at a concentration of 0.5% of the total monomer mass. The mixture was stirred to achieve a homogeneous solution. Vacuum degassing was then performed to remove oxygen and water. The degassed solution was then polymerized in an oven at 70°C for 6 hours. The polymerized gel was then dried in a vacuum oven at 85°C for 72 hours to remove NMP. The obtained polymer was dispersed in dimethoxyethane (DME) at the concentration of 0.2g ml^{-1} and then stirred to obtain a homogeneous solution. The homogeneous solution was dropped onto the lithium foil, allowed to dry overnight, and then degassed under vacuum to obtain the PAM-b-PHFBA coated Li.

Synthesis of CNT-modified carbon cloth

CNT@Ru catalyst or pristine CNT was dispersed in Isopropyl alcohol solution by sonication with 10 wt% Polytetrafluoroethylene (PTFE) as the binder. Cathode was prepared with the carbon papers (Φ 16 mm) being immersed in the positive black suspension above and then dried in a 60 °C oven for 10 min to remove the isopropanol in the dispersion. This process was repeated 3-6 times and finally dried at 110 °C in vacuum for 12 h to obtain a carbon paper positive electrode loaded with 0.5 $mg \cdot cm^{-2}$ of CNT@Ru or CNT.

Preparation of CNT@Ru catalyst

In a weight ratio of 2:1, the carbon nanotubes activated by nitric acid and $RuCl_3 \cdot xH_2O$ were dissolved in water, swirled uniformly for an hour, and then the pH was brought down to 7-8 by applying $NaHCO_3$. After 12 hours of stirring, the solution was centrifuged, washed, and dried overnight to obtain the Ruthenium precursor. The previously mentioned precursor was calcined at 400 °C for 2 h in an argon atmosphere to obtain a high-crystallinity Ru catalyst, with a heating rate of 5 °C/min. The black powder was collected and denoted as CNT@Ru catalyst.

Preparation of Li-O_2 batteries

The Li–O_2 batteries were assembled into a Swagelok-type cell as a sequence of $LiFePO_4$. (Φ 16 mm), a glass fibre separator (Whatman GF/D microfibre filter paper, 2.7-μm pore size), and the prepared carbon cloth as the air electrode. The water content in the pristine solvents of electrolytes is below 50 ppm, as measured by a Karl Fisher titration. The LFP electrode was pre-treated to partly deplete the lithium at a current density of 0.075 $mA \cdot cm^{-2}$ before the LFP-O_2 battery was assembled. After the battery assembly, the batteries were stabilized in an oxygen atmosphere for 0.5 h before testing. The whole process of battery assembly was performed in an Ar-filled glove box (<0.1 ppm of H_2O and 0.1 ppm of O_2).

Charaterizations

Cathode samples were washed with anhydrous DME prior to scanning electron

microscopy (SEM) imaging. All samples were transferred to the SEM chamber by a hermetic transfer box to avoid exposure to the ambient air. The process is to seal the sample platform, remove the seal cover with the help of the vacuum transition chamber added by SEM and the corresponding operation lever, and finally transfer to the shooting area. SEM images were acquired on a GeminiSEM 500 microscope. The micrographs were obtained with a 5 kV voltage. X-ray diffraction (XRD) characterizations were performed on an X'Pert MPD Philips X-ray diffraction meter with filtered Cu Kα radiation (λ = 1.5405 Å). Air-sensitive samples were protected by a Kapton film. ^{1}H-NMR (nuclear magnetic resonance) spectra of electrolytes were collected on a wide cavity solid-state superconducting NMR spectrometer (Bruker AVANCE AV III 400WB). The infrared test is operated by instrument Bruker ALPHA II compact FT-IR spectrometer in a glove box filled with argon. The ionic conductivity of the different electrolytes was measured by electrochemical impedance spectroscopy (EIS) in a frequency range from 100 mHz to 1 MHz with an AC amplitude of 10 mV on a VSP-200 potentiostat/galvanostat station (Bio-logic Science Instruments).

Theoretical Calculation

HOMO and LUMO are calculated by Gaussian16 software with the B3LYP/6-311++g(d,p) basis set[1]. Surface electrostatic potential is displayed by GaussView software at the electron density isosurface value of 0.02 a.u. Mayer bond order was calculated by Multiwfn program[2, 3]. The structures and the change of Gibbs Free Energy of monomers and complexes with PPD and OH^- were optimized at the level of B3LYP/6-311++g(d,p) basis set. All of the optimized structures were confirmed by the absence of negative frequency. The Gibbs free energy change is the value of ΔG according to the integration of the corresponding two monomers. The visualization of the frontier molecular orbitals was rendered using Visual Molecular Dynamic program (VMD), and the isosurface is set to 0.05.

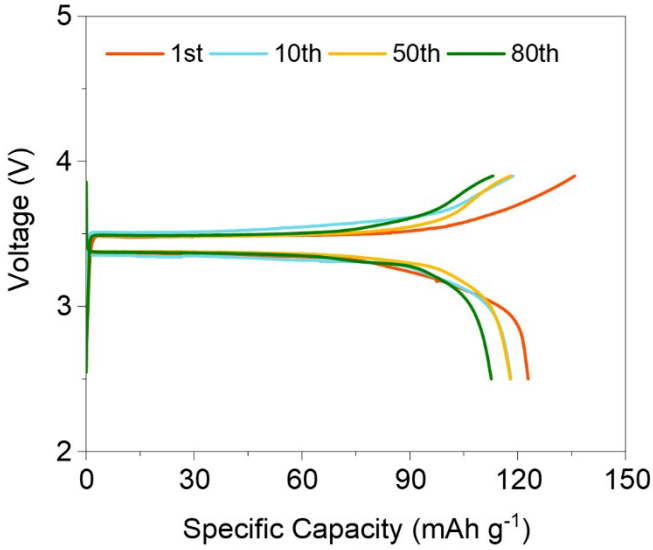

Fig. S1 The discharge and charge profiles of Li-ion cells with $LiFePO_4$ electrode at 15 mA g^{-1}.

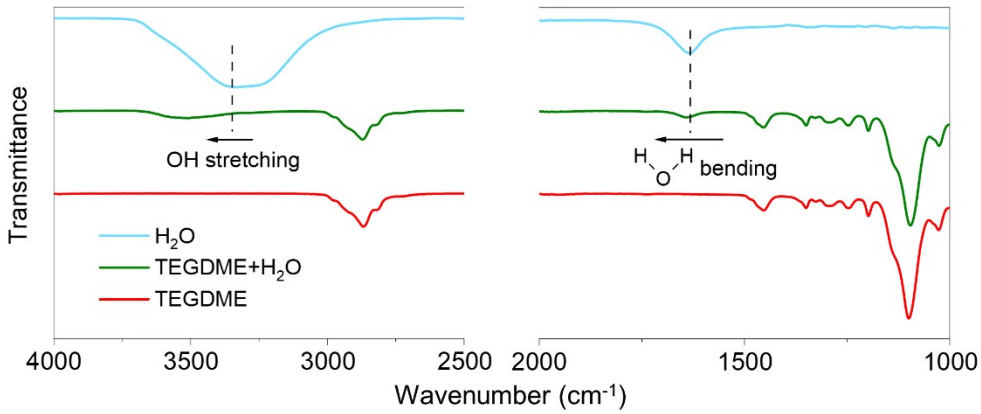

Fig. S2 FTIR of the H_2O, TEGDME, and the mixing electrolyte (2% H_2O).

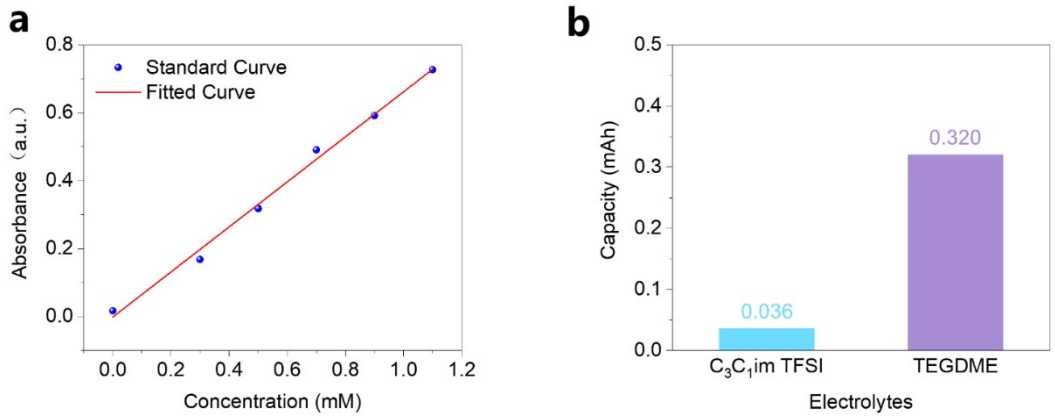

Fig. S3 (a) Standard and fitted curves of O_2^- concentration in titanium oxysulfate detection. (b) Calculated capacity contributions from Li_2O_2 in different solvents with 0.5 M LiTFSI and 6% H_2O.

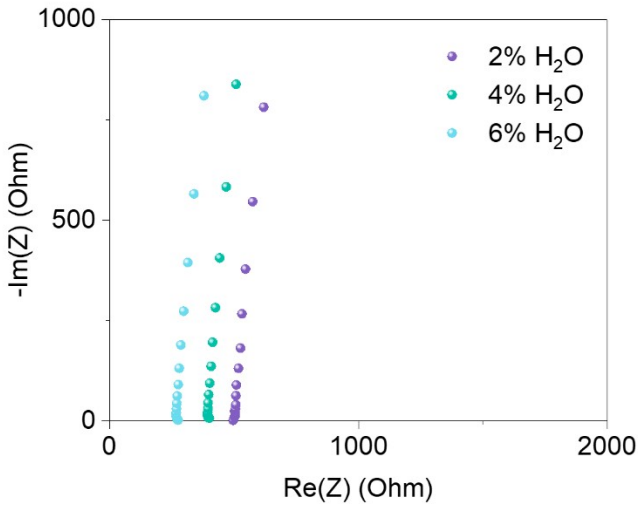

Fig. S4 The ionic conductivity of C_3C_1im TFSI-based electrolyte with different H_2O content.

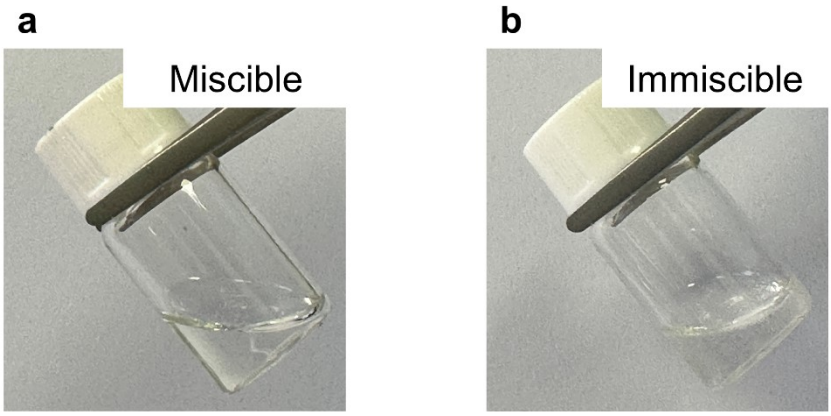

Fig. S5 Photos of C_3C_1im TFSI-based electrolyte with (a) 6% H_2O and (b) 8% H_2O.

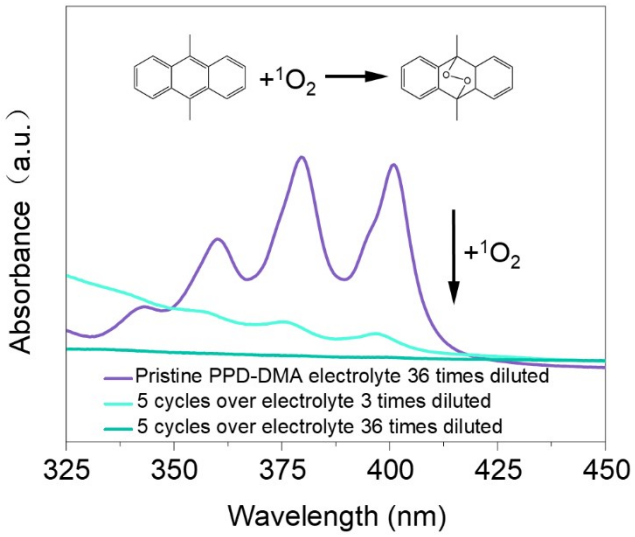

Fig. S6 UV-vis absorption spectrum of DMA in C_3C_1im TFSI-based electrolyte after cycling.

Note: The embedded equation displays the addition reaction of DMA and $^1O_2$.

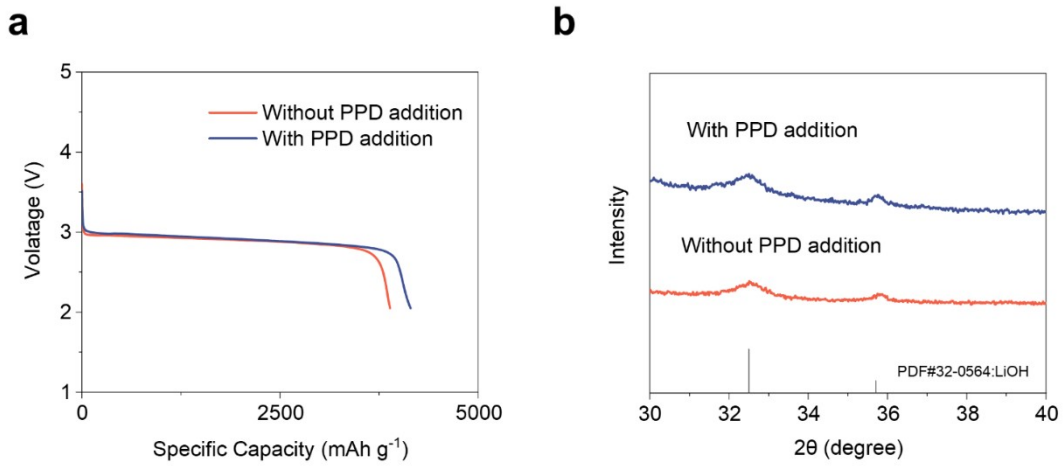

Fig. S7 (a) Discharge performance of electrolytes with or without PPD in C_3C_1im TFSI-based electrolyte with 6% H_2O addition. (b) XRD patterns of the discharged cathode with or without PPD in C_3C_1im TFSI-based electrolyte with 6% H_2O addition.

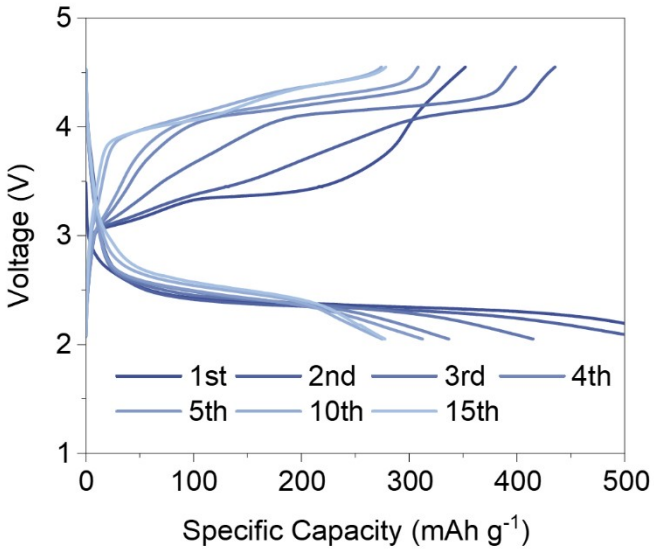

Fig. S8 The cycling performance of the nonaqueous electrolyte based on C_3C_1im TFSI with PPD addition.

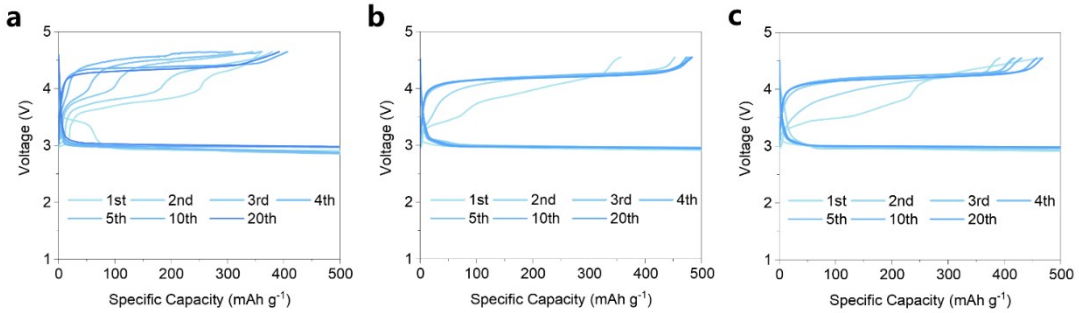

Fig. S9 The cycling performance of electrolytes with different PPD concentrations. The concentrations of PPD in 0.5 M LiTFSI and 6% H_2O content in C_3C_1im TFSI-based electrolyte are in sequence as follows: (a) no PPD addition (b) 25 mM PPD addition, and (c) 50 mM PPD addition.

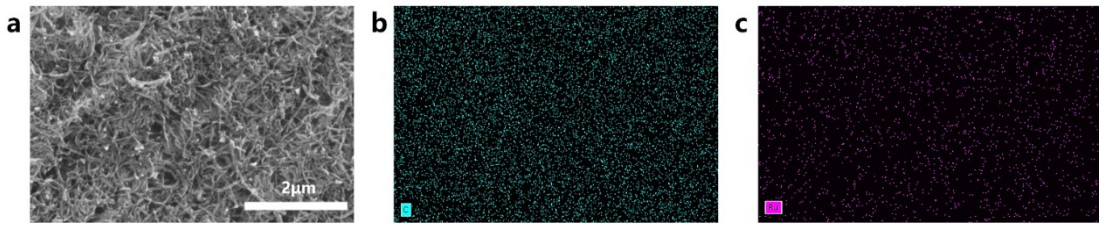

Fig. S10 SEM (a) and EDS (b,c) images of CNT@Ru-modified carbon cloth.

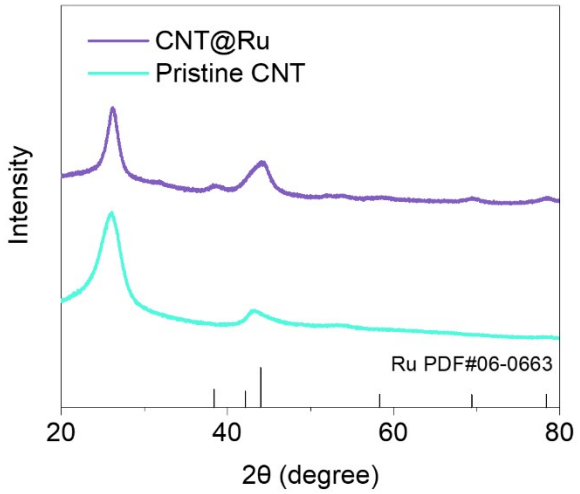

Fig. S11 XRD patterns of the CNT@Ru and pristine CNT powder.

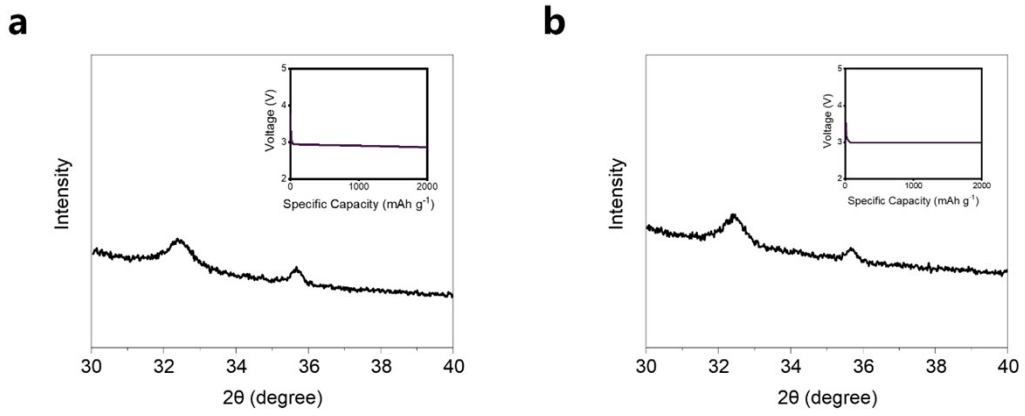

Fig. S12 XRD patterns of the LiOH pre-deposited cathode modified with (a) CNT and (b) CNT@Ru. The embedded image is the discharge pattern of Li-O_2 battery, which was used to obtain LiOH pre-deposited cathodes. Electrolyte is applied with 6% H_2O and no PPD addition.

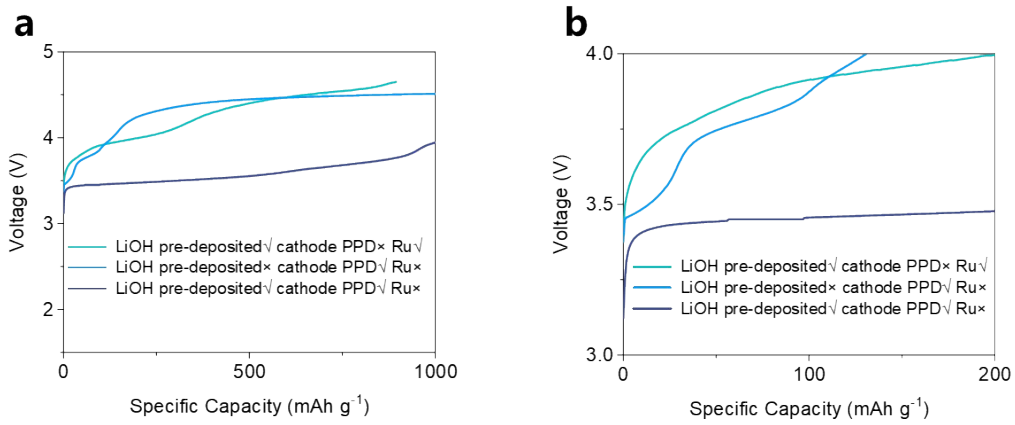

Fig. S13 Charge pattern (a) and magnified pattern (b) of Li-O_2 battery assembled by cathode with or without LiOH deposited and with or without catalyst addition.

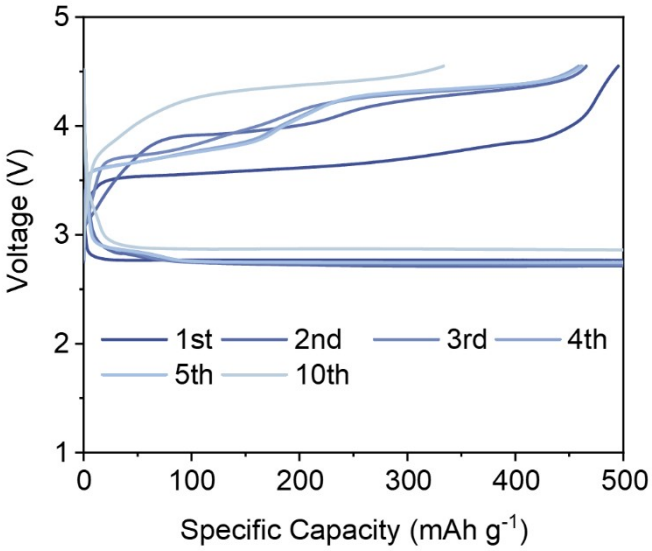

Fig. S14 Cycling performance of Li-O_2 battery in E-PT.

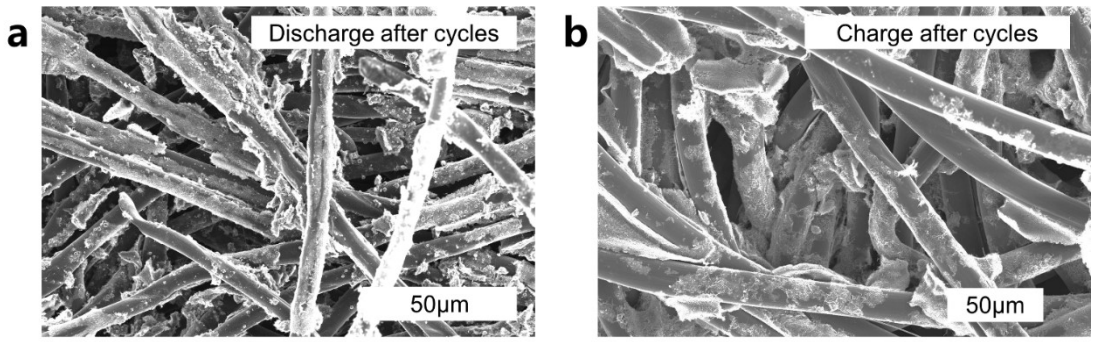

Fig. S15 SEM images of the (a) discharged and (b) charged cathodes in E-PT after 10 cycles at the capacity limitation of 500 mAh g^{-1}.

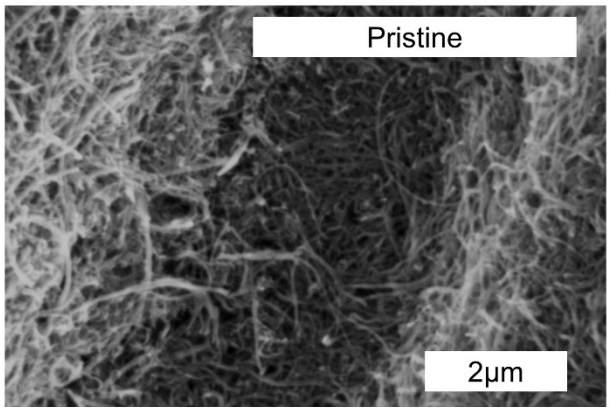

Fig. S16 SEM images of the pristine cathodes.

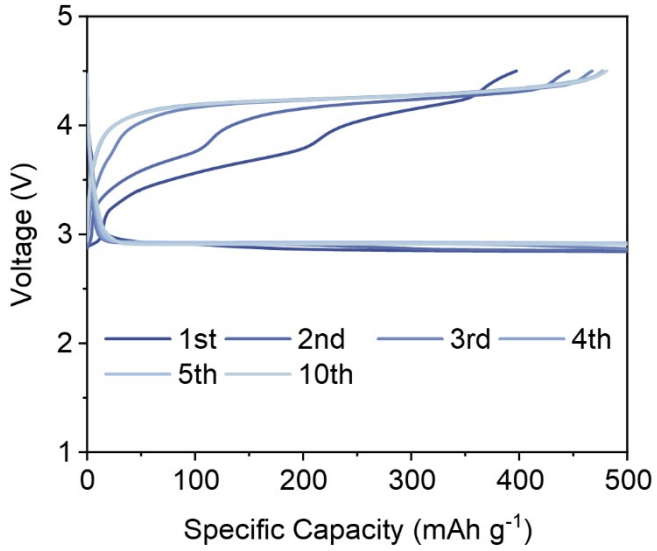

Fig. S17 Cycling performance of Li-O_2 battery in E-PC.

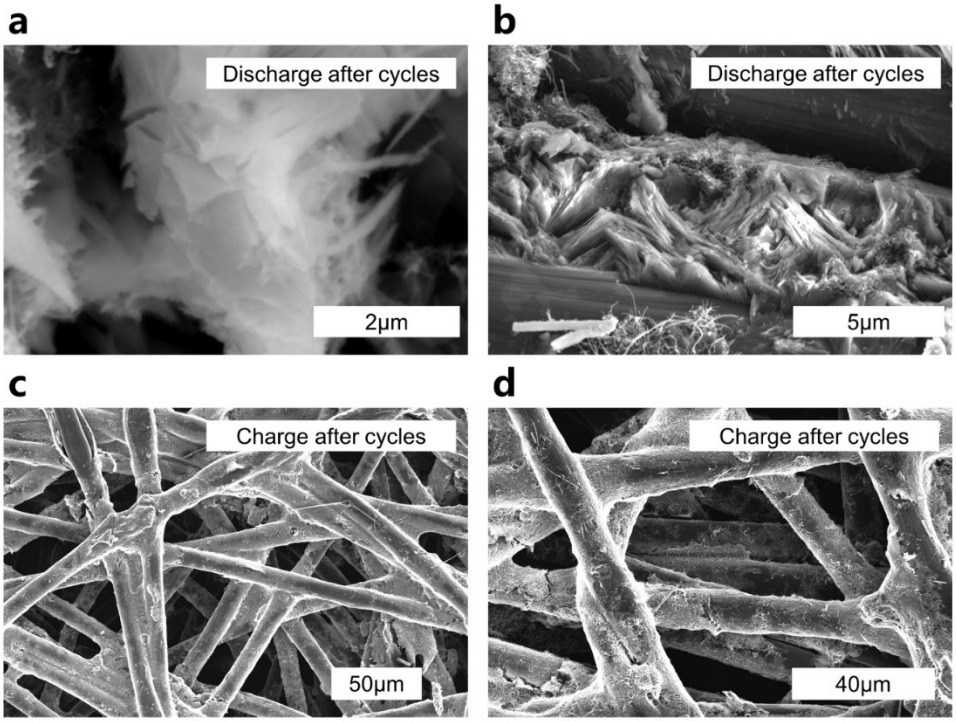

Fig. S18 SEM images of the discharged (a-b) and charged (c-d) cathodes in E-PC after 10 cycles at the capacity limitation of 500 mAh g^{-1}.

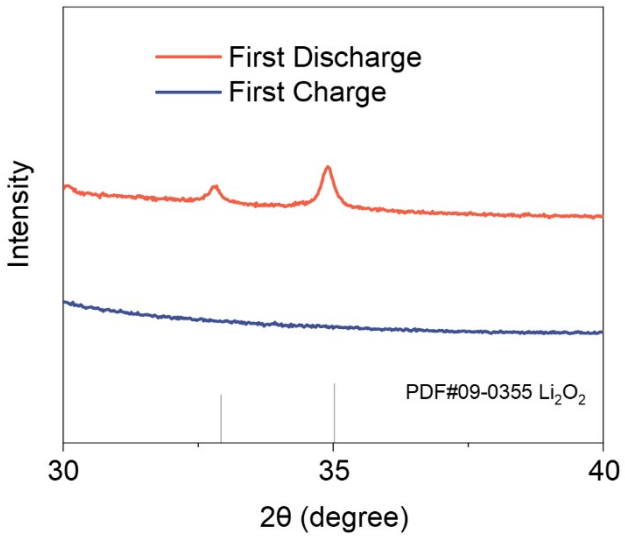

Fig. S19 XRD patterns of the cathode after the first cycle of charge and discharge in E-PT.

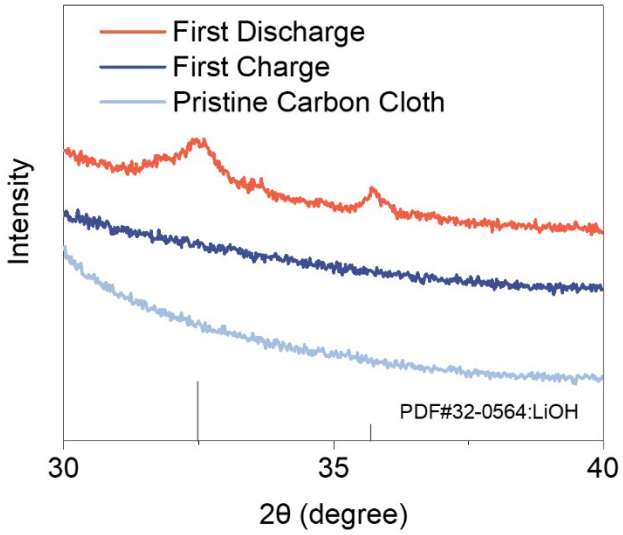

Fig. S20 XRD patterns of the cathode after the first cycle of charge and discharge in E-PC.

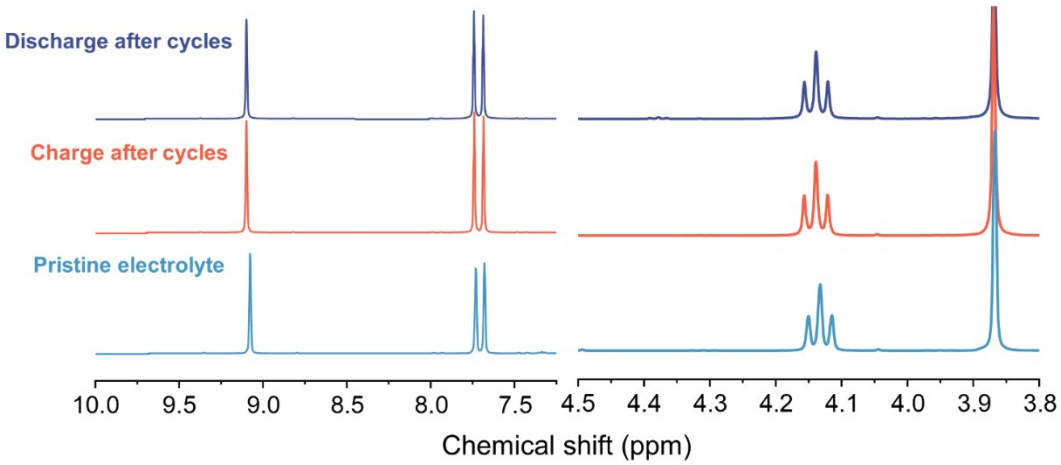

Fig. S21 ^{1}H NMR spectra of E-PC of the pristine electrolyte, the electrolyte after discharging and charging processes following cycles.

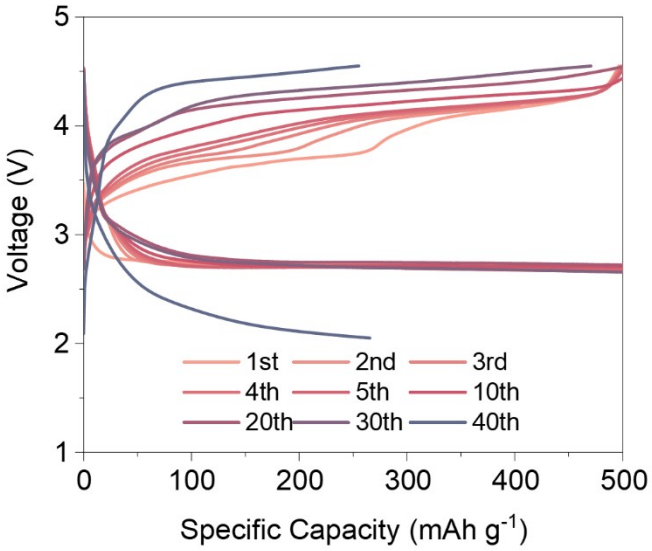

Fig. S22 Cycling performance of Li-O_2 battery with CNT@Ru-modified cathode in C_3C_1im TFSI-based electrolyte without PPD addition, under a current density of 100 mA g^{-1} and cut-off capacity of 500 mA h g^{-1}.

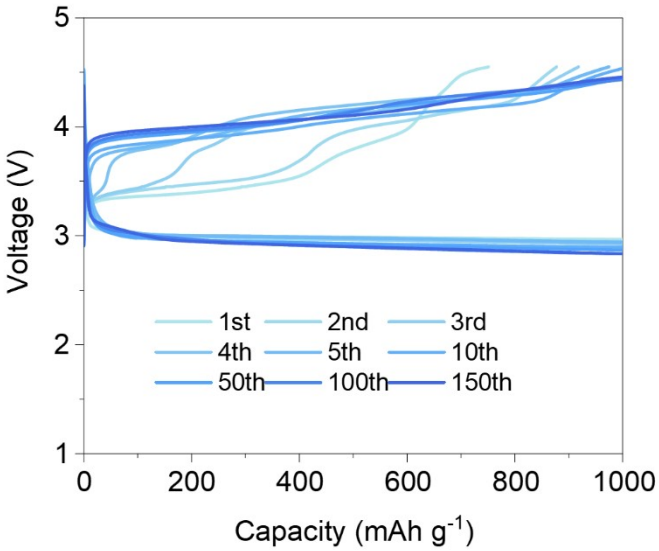

Fig. S23 Cycling performance of Li-O_2 battery with CNT@Ru-modified cathode in C_3C_1im TFSI-based electrolyte with PPD addition, under a current density of 100 mA g^{-1} and cut-off capacity of 1000 mA h g^{-1}.

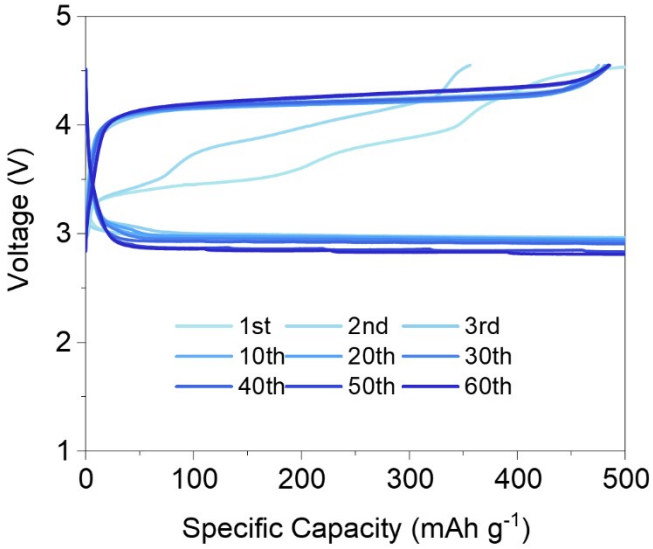

Fig. S24 Prolonged cycling performance of Li-O_2 battery in E-PC to test parasitic products.

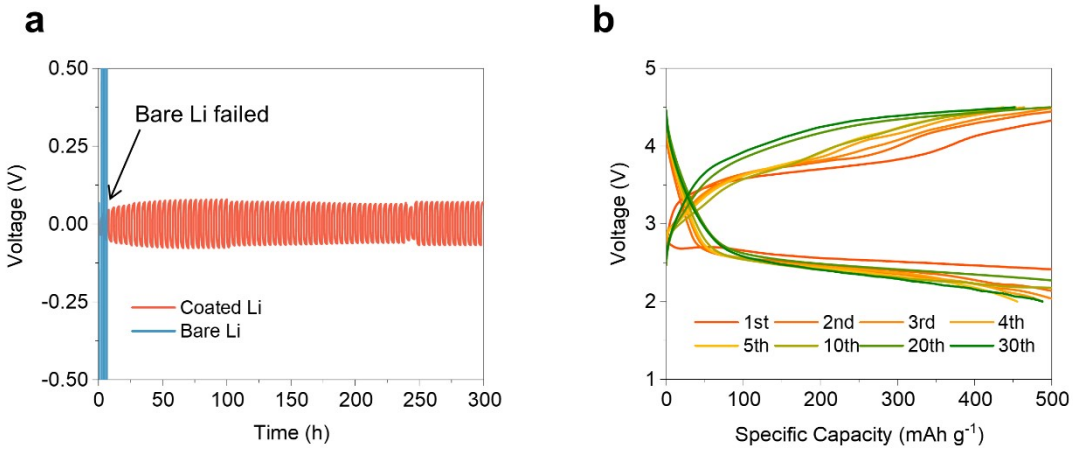

Fig. S25 (a) Cycling performance of PAM-b-PHFBA coated Li||Li cell assembled in C_3C_1im TFSI-based hydrous electrolyte (6% H_2O) at 0.1 mA cm^{-2}. (b) Cycling performance of PAM-b-PHFBA coated Li-O_2 battery with CNT cathode in C_3C_1im TFSI-based hydrous electrolyte (6% H_2O).

Table S1. The energy level of various molecules.

Electrolyte Species	HOMO (eV)	LUMO (eV)
PPD	-5.15466	0.35511
PPD^+	-7.33021	-1.54915
TEGDME	-7.03741	-0.24571
$C_3C_1im^+$	-8.04478	-1.33907

Table S2. Ionic conductivity of C_3C_1im TFSI-based electrolyte with different water content at 25 °C.

Electrolytes	Ionic conductivity (mS cm^{-1})
0.5 M LiTFSI in C_3C_1im TFSI 2% H_2O	0.03216
0.5 M LiTFSI in C_3C_1im TFSI 4% H_2O	0.03985
0.5 M LiTFSI in C_3C_1im TFSI 6% H_2O	0.05794

Table S3. The Mayer bond orders of some covalent bonds obtained by Multiwfn program.

Mayer bond order	C_{10}-N_{12}
PPD	1.02280060
PPD^{+}	1.06508770

Table S4. The energy of OH^- and OH*.

Charge states	OH^-	OH*
Energy (eV)	-2066.5719	-2061.7677

Table S5. The energy of various states with PPD and OH^-.

Charge states	PPD: OH^-	PPD^+: OH^-	PPD: OH*
Energy (eV)	-14139.9788	-14138.6109	-14138.9802

References:

1 Frisch, M. J. e.; Trucks, G. W.; Schlegel, H. B.; Scuseria, G. E.; Robb, M.; Cheeseman, J. R.; Scalmani, G.; Barone, V.; Petersson, G. A.; Nakatsuji, H., Gaussian 16. Gaussian, Inc. Wallingford, CT: 2016.

2 T. Lu,F. Chen, J. Comput. Chem. 2012, 33, 580-592

3 I. Mayer, Chem. Phys. Lett. 1983, 97, 270-274.